Spherulitic Structure Development During Crystallization in a Finite Volume

E. Piorkowska,[1] N. Billon,[2] J. M. Haudin,[2] J. Kolasinska[1]

[1]*Centre of Molecular and Macromolecular Studies, Polish Academy of Sciences, 90 363 Lodz, Poland*
[2]*Ecole des Mines de Paris, Centre de Mise en Forme des Materiaux, UMR CNRS 7635, BP 207, 06 904 Sophia Antipolis, France*

Received 25 April 2001; accepted 11 February 2002

ABSTRACT: This study was devoted to the formation of a spherulitic pattern in a confined space. Thin poly(methylene oxide) films, one wide and the second of width of average spherulite diameter, were crystallized isothermally at the same temperature and studied. In the narrow sample, the number of spherulites per unit area increased, whereas the length of interspherulitic boundary lines per unit area and the number of triple points, impingement points of three spherulites, per unit area were significantly smaller than in the wide sample. Computer simulation of the spherulitic crystallization demonstrated not only a decrease in the number of boundary lines and triple points per unit area due to limits of space available for the spherulitic nucleation and growth but also differences in the progression of the spherulitic structure formation between wide films and narrow strips. A model of the spherulitic pattern development in narrow strips of the polymer based on probability theory is elaborated. The model allows one to predict the rates of formation of the interspherulitic boundaries and also the distributions of distances from the spherulites centers to the boundaries for an isothermal and a nonisothermal crystallization. The total length of interspherulitic lines and the total number of triple points between spherulites can be also calculated. © 2002 Wiley Periodicals, Inc. J Appl Polym Sci 86: 1373–1385, 2002

Key words: crystallization; spherulitic structure; finite volume; modeling

INTRODUCTION

Spherulitic structure is an important factor affecting the properties of crystalline polymeric materials. Interspherulitic boundaries and multiple boundary points, which are weak spots of structure, influence ultimate mechanical properties and gas sorption phenomena, among other things.[1,2]

The theory describing the development of the spherulitic structure deals primarily with a conversion of a melt into spherulites. The theory initiated by Avrami and Evans's[3,4] formulations for isothermal crystallization in an infinite body was developed later to describe more complex processes such as nonisothermal crystallization,[5,6] crystallization in a confined volume,[7–11] including also transcrystallinity effects,[12] and crystallization in fiber-reinforced composites.[13] In an infinite body, conversion degree depends on time (t) elapsed from the beginning of crystallization in the known way $1 - \exp[-E_\infty(t)]$, where the second component is the probability that an arbitrarily chosen sample point will remain at time t outside of any spherulite. E_∞ is determined by the time dependencies of the nucleation rate [$F(t)$] and growth rate [$G(t)$] of the spherulites[6]:

$$E_\infty(t) = k\pi \int_0^t F(\tau)\left[\int_\tau^t G(s)\, ds\right]^n d\tau \qquad (1)$$

where k and n equal 1 and 2, respectively, in a two-dimensional case and 4/3 and 3, respectively, in a three-dimensional case.

When a limited polymer portion in the form of a plate or a strip of film is considered, the conversion degree equals $1 - \exp[-E(t, s_1, s_2)]$ and depends on distances s_1 and s_2 from both polymer borders. E can be expressed as the difference[8–10]

$$E(t, s_1, s_2) = E_\infty(t) - E_1(t, s_1) - E_1(t, s_2) \qquad (2)$$

where the subtraction of $E_1(t, s_1)$ and $E_1(t, s_2)$ is due to the lack of spherulites beyond the material borders. Hence, the limitation of volume slows down the conversion of the melt. An additional spherulitic nucleation at the polymer borders accelerates the conversion. To describe the kinetics of the conversion in this case, it is necessary to add appropriate components to the right side of eq. (2).[10–12]

Correspondence to: E. Piorkowska (epiorkow@bilbo.cbmm.lodz.pl).

Contract grant sponsor: PICS program (SCSR-CNRS), with French–Polish cooperation.

Although the computer simulation allows one to visualize the spherulitic structures crystallized not only in infinite bodies but also in confined spaces[8,9,11,12] and in fiber-reinforced composites,[13–15] the efforts to describe mathematically the formation of interspherulitic borders has been limited to crystallization apart from the material limits.[16–19] They were based on considerations of the probability of the occurrence of nucleation events in space and in time, resulting in contacts of respective numbers of crystallizing fronts. The derived time dependence of the formation of multiple boundary points allowed for the prediction of the time distribution of an acoustic emission recorded during the crystallization of isotactic polypropylene and poly(methylene oxide) (POM).[20] The source of the recorded ultrasound was a cavitation in a polymer melt confined between spherulites; in the occluded pocket of melt, the cavitation occurred shortly before the formation of the multiple boundary points inside this pocket.

Because the vicinity of the polymer border has an effect on the rate of conversion of the polymer melt into the spherulites, one can expect that it also influences the development of the interspherulitic boundaries and the final spherulitic pattern.

This article is devoted to this latter point in the case of POM. A probabilistic model allowing for description of the evolution of interspherulitic boundaries in the vicinity of spatial limits of the polymer is described. We also conducted computer simulation of spherulitic structures[21] as an independent method of obtaining the data describing the interspherulitic boundaries as a function of the polymer film width and to verify predictions of the mathematical model.

EXPERIMENTAL

As this study dealt with a two-dimensional approach to crystallization, we had to use very thin samples. The polymer used was POM Tarnoform 300 (Zaklady Azotowe w Tarnowie SA, Tarnow, Poland) with a melt flow index of 9 ± 1 g/10 min (190°C, 2.16 kg). Films (2 μm thick) were obtained through casting on microscopic cover glasses from a 2% solution of the polymer in dimethylformamide.

Samples were melted at 190°C for 3 min, cooled down at a rate of 10°C/min to 150°C, and then crystallized isothermally in a Linkam (Waterfield, UK) hot stage under a continuous flow of nitrogen. The crystallization was monitored by a light microscope, connected with a CCTV camera, a display, a VHS video recorder, and a computer. After the completion of the crystallization, the samples were photographed part by part by means of the camera connected with the computer. The magnified images were printed and glued together for measurements. To minimize the potential effect of variable thicknesses of the film, the samples were cut from a single specimen. The parallel strips were formed by removal of the material between them. This was achieved with a razor blade under magnification, obviously before melting. The width of strips selected for further studies varied between 0.23 and 0.25 mm, with an average of 0.24 mm. The roughness of the edges allowed for the measurement of the local strip width with an accuracy of 0.02 mm. The width represented approximately one spherulite diameter. The total length of the strips was 12.3 mm. As a wide sample, a rectangle (6.4×1.9 mm^2) was chosen in the vicinity of the strips but 0.5 mm apart from the boundary of the polymer. Because the rectangle could be treated as a parallel composition of several narrow strips joined together, the rectangular shape of the wide sample had no influence on the obtained results. Both of the two areas, the wide and the narrow, were examined.

For characterization of morphology, the number of spherulite centers, the number of triple points at which three spherulites met, and the length of boundary lines between pairs of spherulites were measured. The spherulitic pattern could also be characterized by the distribution of distances from the centers of the spherulites to the boundaries formed by these spherulites with neighbors.[19] Hence, distances were measured from the centers of spherulites to points where these spherulites impinged with two others in both the narrow and the wide sample, and the distributions of distances were calculated.

EXPERIMENTAL RESULTS

Figure 1(a,b) depicts the microphotographs of fragments of the wide sample and the strip, respectively. Besides straight line boundaries, hyperbolic boundaries between two neighboring spherulites were also found in both samples, the wide and the narrow, indicating not entirely instantaneous nucleation. There was no evidence for edge nucleation, as nuclei were mainly distributed inside the strip.

The wide sample contained 249 spherulite centers, 471 triple points, and 90.07 ± 1.8 mm of boundary lines, hence 20.58 centers, 39.75 points, and 7.44 ± 0.15 mm of lines per square millimeter. For strips, the respective values were 75 spherulites, 48 points, and 16.46 ± 0.33 mm of boundary lines, which gave 25.38 ± 0.5 centers, 16.24 ± 0.33 points, and 5.57 ± 0.22 mm of lines per square millimeter. The errors in the determination of the numbers of centers and triple points per unit area of the narrow strip originated primarily from the accuracy of the estimation of the strip width due to the roughness of the strip borders. In the case of the interspherulitic lines, the accuracy of length measurements also contributed to the error. A detailed discussion of the influence of the numbers of centers and triple points considered on the calculated average

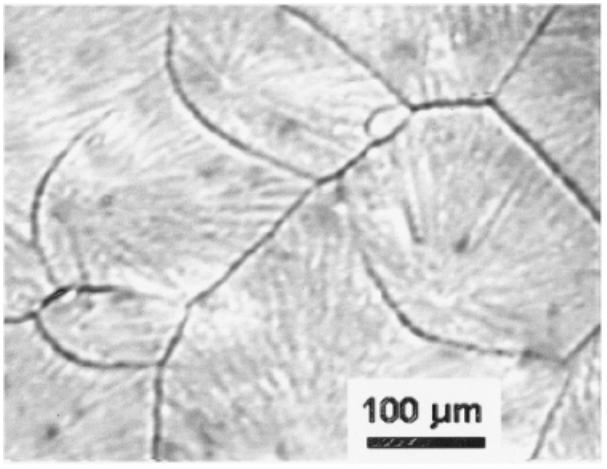

(a)

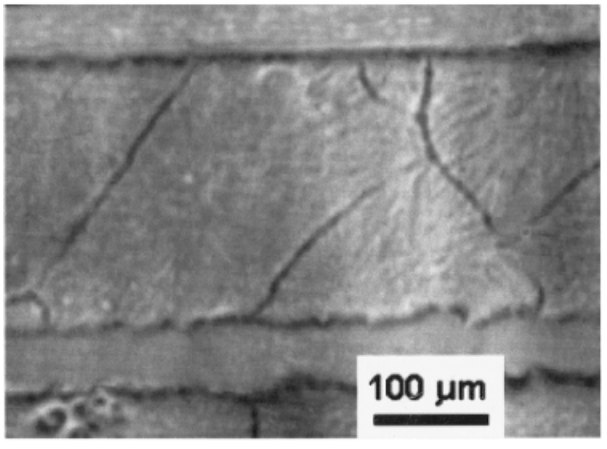

(b)

Figure 1 Micrographs of fragments of POM (a) wide film and (b) narrow film.

values based on the probability theory is conducted in Appendix B. The average spherulite radius in the wide sample was 0.11 mm. To determine the distributions of distances from spherulite centers to impingement points of these spherulites with their neighbors, we measured 129 distances in the strips and 540 distances in the wide sample. The normalized histograms of the distances from the centers to the contact points of three spherulites are plotted in Figure 2. The distribution of distances in the narrow sample had a higher fraction of shorter distances, and the fraction of the largest distance was reduced.

The results clearly show the influence of finite sample width on the microstructure. The number of spherulites per unit area was greater in the narrow sample, whereas the length of boundary lines and the number of triple points per unit area were smaller compared with the respective values for the wide sample.

PROBABILISTIC MODEL

In ref. 17, the application of the probability theory to the characterization of the spherulitic pattern development during isothermal and nonisothermal crystallization in infinite samples is depicted.

In this section, the formation of interspherulitic boundaries during crystallization in strip of a thin film is described by means of probability theory. Two types of nucleation processes are considered: instantaneous nucleation and sporadic nucleation at a time-dependent nucleation rate. Additionally, we assumed that the spherulite growth rate has the same momentary value in the entire film.

Instantaneous Nucleation

During two-dimensional spherulitic crystallization, the boundary between two neighboring spherulites has the form of a line, whereas three spherulites come to contact at a point. The probability of the formation of a contact point between four spherulites on a plane can be neglected.[17]

In the case of instantaneous nucleation, the probability for a point to be included in a boundary is only constrained by geometrical factors. Let us consider an arbitrarily chosen point A in a strip of width 2 h (Fig. 3). The boundary between two spherulites passes through point A on the condition that the distances (r) from both spherulite centers to point A are equal with the accuracy of an infinitely small dr, and that no other spherulite is nucleated around point A within a distance r. That means that (1) two spherulites have to be nucleated inside a fictitious ring of radius r and width dr (Fig. 1) at angles φ_1 and φ_2 [strictly at angles within the ranges (φ_1; $\varphi_1 + d\varphi_1$) and (φ_2; $\varphi_2 + d\varphi_2$), respec-

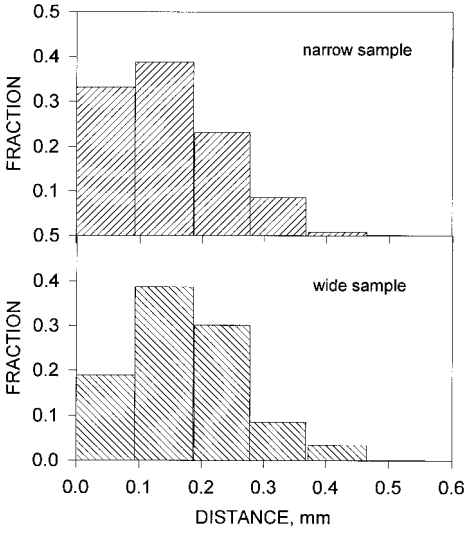

Figure 2 Distributions of distances from the spherulite centers to triple boundary points in narrow and wide POM samples.

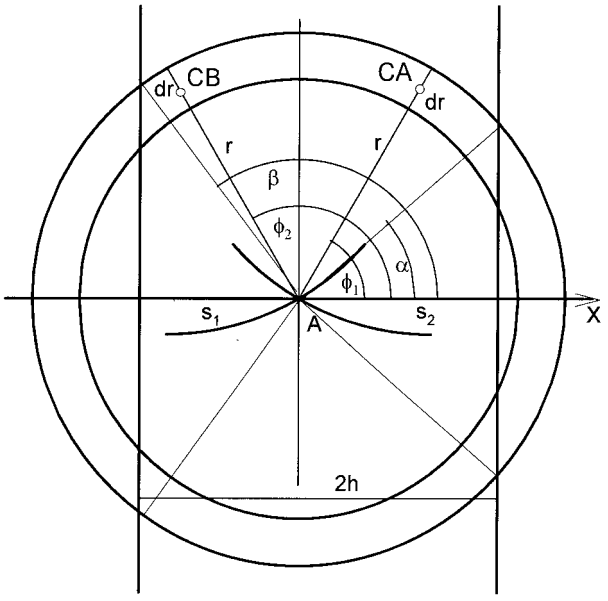

Figure 3 Schematic location of spherulite centers around an arbitrarily chosen point in the film.

tively] with respect to the x axis, and (2) no other spherulite can be nucleated inside a circle of radius r around point A. For the strip, only the part of the circle between the strip borders has to be considered.[10] The surface area (S) of this part of the circle equals

$$S(r, s_1, s_2) = \pi r^2 - W(r, s_1) - W(r, s_2) \quad (3a)$$

where $s_2 = 2h - s_1$ and $W(r, s_1)$, and $W(r, s_2)$ denote the parts of circle truncated by the sample borders at distances s_1 and s_2, respectively, from point A. For $r < s$

$$W(r, s) = 0,$$

and for $r > s$

$$W(r, s) = \arctan[(r^2/s^2 - 1)^{0.5}]r^2 - s(r^2 - s^2)^{0.5} \quad (3b)$$

According to the Poisson law, the probabilities of event (1) and event (2) are expressed in the form $\exp(-D\ rdr\ d\varphi_1)(D\ rdr\ d\varphi_1)\exp(-D\ rdr\ d\varphi_2)(D\ rdr\ d\varphi_2)$ and $\exp\{-D[S(r, s_1, s_2) - rdr(d\varphi_1 + d\varphi_2)]\}$, respectively, where D is the spherulite nucleation density, that is, the number of nuclei per unit area of a film and $rdr\ d\varphi_1$ and $rdr\ d\varphi_2$ are the area elements in which the spherulite centers are nucleated. The probability, P_2, that the interspherulitic boundary is formed at distances r from two spherulite centers located at angles φ_1 and φ_2 is a product of the probabilities of event (1) and event (2):

$$P_2(r)dr\ d\varphi_1\ d\varphi_2 = \exp[-DS(r, s_1, s_2)](Drdr)^2\ d\varphi_1\ d\varphi_2 \quad (4)$$

Different radial locations of spherulite centers within the ring result in different positions of the spherulitic fronts and, thus, of the interspherulitic boundary, which is shown in Figure 4. When one center is at CB_1 and the second one is between CA_1 and CA_2, the fronts are in contact at the arc between A and C_x, which can be approximated by AC. Considering all possible positions of the centers, one concludes that the interspherulitic boundary is confined to the tetragon ACA′C′ having the surface area $da = dr^2(2 \sin \omega \cos \omega)^{-1}$, where $\omega = 0.5|\varphi_2 - \varphi_1|$. Thus, eq. (4) expresses the probability for the boundary between two spherulites to be created within da. The boundary between two spherulites nucleated at the same time is a straight line bisecting the angle $2\omega = \varphi_2 - \varphi_1$. In the situation drawn in Figure 4, the boundary line passes through the points A and A′; $AA' = dl = dr(\cos \omega)^{-1}$. Thus, the average width of the boundary equals $dw = dr(2 \sin \omega)^{-1}$. Dividing $P_2(r)dr\ d\varphi_1\ d\varphi_2$ by the width (dw), one calculates the probability, f_2, of the formation of the boundary length (dl) at distance r from each of the spherulite centers confined to angles $d\varphi_1$ and $d\varphi_2$:

$$f_2(r, \varphi_1, \varphi_2, s_1, s_2)dr\ d\varphi_1\ d\varphi_2 = \exp[-DS(r, s_1, s_2)] \times (Dr)^2 2 \sin(0.5|\varphi_2 - \varphi_1|)dr\ d\varphi_1\ d\varphi_2 \quad (5)$$

Triple points are always at intersections of boundary lines. The triple point is formed at point A at a distance r apart from the three spherulite centers on the following condition: these three spherulites have

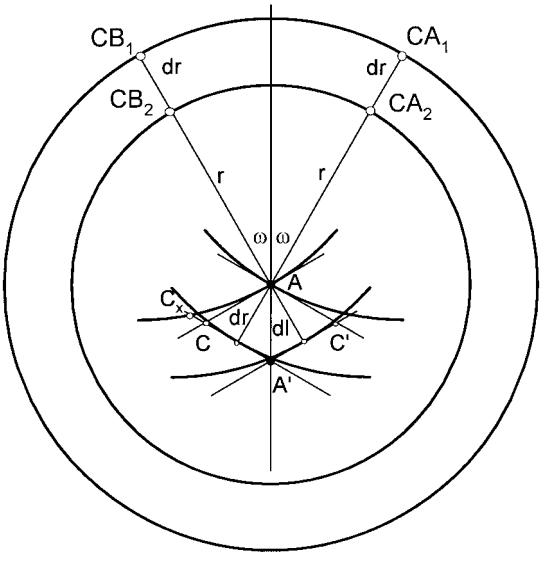

Figure 4 Scheme of the possible positions of the spherulite centers within the ring width dr and their influence on the location of the contact point of spherulite fronts.

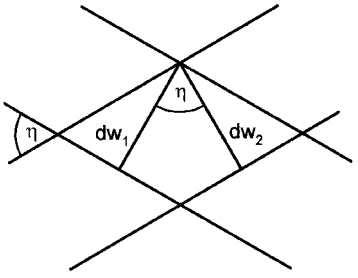

Figure 5 Superposition of two interspherulitic boundaries leading to formation of triple point.

to be nucleated inside the ring of radius r and of the width dr at angles φ_1, φ_2, and φ_3 that is within the area elements $rdr\,d\varphi_1$, $rdr\,d\varphi_2$, and $rdr\,d\varphi_3$. In addition, no other spherulite can be nucleated inside the circle of radius r around point A. Hence, the probability of the triple point formation is

$$P_3(r, s_1, s_2)dr\,d\varphi_1\,d\varphi_2\,d\varphi_3 = \exp[-DS(r, s_1, s_2)] \times (Drdr)^3 d\varphi_1\,d\varphi_2\,d\varphi_3 \quad (6)$$

The consequence of the various radial centers' positions within dr can be estimated by analysis of the superposition of two boundaries having the widths $dw_1 = dr(2\sin\omega)^{-1}$ and $dw_2 = dr(2\sin\omega')^{-1}$, where $\omega' = 0.5|\varphi_3 - \varphi_2|$ (Fig. 5). The angle η between the normals to these boundaries equals $\omega - \omega' = 0.5|\varphi_3 - \varphi_1|$. Thus, the triple point is enclosed in the tetragon in Figure 5 having an area of $dv = dr^2[4\sin(0.5|\varphi_1 - \varphi_2|)\sin(0.5|\varphi_3 - \varphi_2|)\sin(0.5|\varphi_3 - \varphi_1|)]^{-1}$. To obtain the number of the triple points between spherulites with the centers at distances r from these points and at the angles $d\varphi_1$, $d\varphi_2$, and $d\varphi_3$, one has to divide eq. (6) by dv

$$f_3(r, \varphi_1, \varphi_2, \varphi_3, s_1, s_2)dr\,d\varphi_1\,d\varphi_2\,d\varphi_3 = 4\exp[-DS(r, s_1, s_2)](Dr)^3\sin(0.5|\varphi_1 - \varphi_2|)\sin \times (0.5|\varphi_3 - \varphi_2|)\sin(0.5|\varphi_3 - \varphi_1|)]dr\,d\varphi_1\,d\varphi_2\,d\varphi_3 \quad (7)$$

The integration of eqs. (5) and (7) over the ranges $\alpha < \varphi_i < \beta$ for $i = 1 \ldots n$, where $n = 2$ for eq. (5) and $n = 3$ for eq. (7), gives access to the length of boundary lines and the number of triple points per unit surface area of the sample at distances r from spherulite centers located within the angle β–α around the considered boundary elements. In the strip of finite width, the two ranges of angle are available for spherulite centers (1) from α to β and (2) from α' to β' (Fig. 3); determined by the distances r, s_1, and s_2, $\alpha = 0$ for $r < s_2$, and $\alpha = \arctan\{[(r/s_2)^2 - 1]^{0.5}\}$ for $r > s_2$, $\beta = \pi$ for $r < s_1$, and $\beta = \pi - \arctan\{[(r/s_1)^2 - 1]^{0.5}\}$ for $r > s_1$, $\alpha' = 2\pi - \beta$, and $\beta' = 2\pi - \alpha$. All possible combinations of centers positions have to be considered, and for n centers within the same angle range, the result of integration should be divided by $n!$ to avoid multiple counting of the same events. Finally, the expressions for the boundary length, F_2, and the number of triple points, F_3, per unit surface area of the sample at distance r from spherulites centers take the forms

$$F_2(r, s_1, s_2)dr = 2U_2(Dr)^2\exp[-DS(r, s_1, s_2)]\,dr \quad (8a)$$

$$F_3(r, s_1, s_2)dr = 4U_3(Dr)^3\exp[-DS(r, s_1, s_2)]\,dr \quad (8b)$$

where U_2 and U_3 are the results of the integration over the angles

$$U_2 = 4\{(\beta - \alpha) - 2\sin[0.5(\beta - \alpha)] + 2\sin[0.5(\beta + \alpha)] - \sin\alpha - \sin\beta\} \quad (9a)$$

$$U_3 = 2[(\beta - \alpha)^2/4 + \cos(\beta - \alpha) - 1 + 0.25(\beta - \alpha) \times \sin(\beta - \alpha)] + 0.5(\beta - \alpha)[(\beta - \alpha) - \sin(\beta - \alpha) + (\sin 2\beta - \sin 2\alpha)] + \cos 2\alpha + \cos 2\beta - 2\cos(\beta + \alpha) \quad (9b)$$

In the case of instantaneous nucleation, the distance from spherulite centers to the boundary formed by these spherulites is always $r = \int_0^t G(t)\,dt$, where t denotes the time of boundary formation and $G(t)$ is the time-dependent growth rate. Hence, substituting this integral for r and $G(t)\,dt$ for dr in eqs. (8a) and (8b), one obtains the rate of interspherulitic lines formation, $H_2(t, s_1, s_2)$, and the rate of triple points formation, $H_3(t, s_1, s_2)$, in unit area of the film at distances s_1 and s_2 from the sample boundaries. For the isothermal crystallization when G is a constant, they are

$$H_2(t, s_1, s_2)\,dt = F_2(Gt, s_1, s_2)G\,dt \quad \text{and} \quad H_3(t, s_1, s_2)\,dt = F_3(Gt, s_1, s_2)G\,dt \quad (10a)$$

The distribution of distances from spherulites centers to the boundary lines between these spherulites, $R_2(r, s_1, s_2)$, and the distribution of distances from the spherulites centers to the triple impingement points formed by these spherulites, $R_3(r, s_1, s_2)$, are obtained by the multiplication of the functions F_2 and F_3 by the number of the spherulites participating in the formation of the respective structure element:

$$R_2(r, s_1, s_2)\,dr = 2F_2(r, s_1, s_2)dr \quad \text{and} \quad R_3(r, s_1, s_2)\,dr = 3F_3(r, s_1, s_2)\,dr \quad (10b)$$

Time-dependent Nucleation Rate

In the case of the sporadic nucleation of spherulites, the interspherulitic boundary is formed between n (2 or 3) spherulites at time t [strictly in time interval $(t - dt, t)$] if their nucleation times, τ, and the distances

from their centers to the boundary (line or triple point), r_i, fulfill the condition[16,17]

$$\int_0^t G(t')\,dt' = \int_0^\tau G(t')\,dt' + r_i \quad \text{for} \quad i = 1 \ldots n \tag{11}$$

which has the simple form $t = \tau + r_i/G$ for isothermal crystallization.

Therefore, we have to calculate the probability that n spherulites are nucleated at times τ_i [strictly in time intervals $(\tau_i; \tau_i + d\tau_i)$], $i = 1 \ldots n$, in rings of radii r_i and of width dr at certain angles φ_i around the arbitrarily chosen point and that no other spherulite is nucleated in subsequent time intervals $d\tau$ until time t in circles of radii $r(\tau, t) = \int_\tau^t G(t')\,dt'$. Because the circles can be truncated by the sample borders, only parts of them are considered, having the surface area $S[r(\tau, t), s_1, s_2]$ as it is expressed by eqs. (3a) and (3b).

Applying the similar reasoning as for the instantaneous nucleation, one gets the expressions for the probabilities of the formation of a boundary between two and between three spherulites:

$$P_2'(t, \tau_1, \tau_2, s_1, s_2)\,dt d\varphi_1 d\varphi_2 = \exp\left[-\int_0^t F(\tau) S[r(\tau, t), s_1, s_2]\,d\tau\right][F(\tau_1) r(\tau_1, t)\,dr] \times [F(\tau_2) r(\tau_2, t)\,dr]\,d\varphi_1\,d\varphi_2 \tag{12a}$$

$$P_3'(t, \tau_1, \tau_2, s_1, s_2)\,dt\,d\varphi_1\,d\varphi_2\,d\varphi_3 = \exp\left[-\int_0^t F(\tau) S[r(\tau, t), s_1, s_2]\,d\tau\right][F(\tau_1) r(\tau_1, t)\,dr] \times [F(\tau_2) r(\tau_2, t)\,dr][F(\tau_3) r(\tau_3, t)\,dr]\,d\varphi_1\,d\varphi_2\,d\varphi_3 \tag{12b}$$

where $F(t')$ denotes the time-dependent nucleation rate.

If there is a time lag between the moments of nucleation of two spherulites, the boundary between them is a hyperbola with the spherulite centers as foci. The radii connecting the foci to any point of the hyperbola are at the same angle with respect to a tangent to this curve. Hence, the momentary direction of the interspherulitic line is always bisecting the angle equal to $\varphi_2 - \varphi_1$. Therefore, the calculation of the length of interspherulitic lines or the number of triple points between spherulites can be done in the same way as for the instantaneous nucleation, that is, by dividing eq. [12(a,b)] by dw and dv, respectively.

Both the radius of the ring and the angle range around point A in which spherulites participating in the formation of the boundary can be nucleated depend on their nucleation time: $\alpha_i < \varphi_i < \beta_i$ and $\alpha_i' < \varphi_i < \beta_i'$: $\alpha_i = 0$ for $r(\tau_i, t) < s_2$ and $\alpha_i = \arctan\{[(r(\tau_i, t)/s_2)^2 - 1]^{0.5}\}$ for $r(\tau_i, t) > s_2$, $\beta_i = \pi$ for $r(\tau_i, t) < s_1$ and $\beta_i = \pi - \arctan\{[(r(\tau_i, t)/s_1)^2 - 1]^{0.5}\}$ for $r(\tau_i, t) > s_1$, $\alpha_i' = 2\pi - \beta_i$ and $\beta_i' = 2\pi - \alpha_i$. Therefore, it is necessary to perform n integrations over the ranges $\alpha_i < \varphi_i < \beta_i$ and $\alpha_i' < \varphi_i < \beta_i'$ for $i = 1 \ldots n$. To obtain the expression for the length of interspherulitic lines and the number of triple points formed at distances s_1 and s_2 from the sample borders at time t by the spherulites nucleated at any moment until t, one has to integrate P_n' over the ranges $0 < \tau_i < t$ for $i = 1 \ldots n$ and to divide the result by $n!$ to avoid multiple counting of the same events. Hence

$$H_2(t, s_1, s_2)\,dt = (2!)^{-1}\exp\left[-\int_0^t F(\tau) S[r(\tau, t), s_1, s_2]\,d\tau\right] \times \left[\int_0^t \int_0^t F(\tau_1) r(\tau_1, t) F(\tau_2) r(\tau_2, t) V_2(\tau_1, \tau_2)\,d\tau_2\,d\tau_1\right] G(t)\,dt \tag{13a}$$

$$H_3(t, s_1, s_2)\,dt = (3!)^{-1}\exp\left[-\int_0^t F(\tau) S[r(\tau, t), s_1, s_2] d\tau\right] \left[\int_0^t \int_0^t \int_0^t F(\tau_1) r(\tau_1, t) F(\tau_2) r(\tau_2, t) F(\tau_3) r(\tau_3, t) \times V_3(\tau_1, \tau_2, \tau_2)\,d\tau_1\,d\tau_2\,d\tau_2\right] G(t)\,dt \tag{13b}$$

where the expressions for functions V resulting from the integration over the angles φ_i are given in Appendix A.

The functions H describe the rates of formation of boundary elements in unit area of the sample at distances s_1 and s_2 from the sample boundaries. The distributions of distances r from spherulite centers to boundaries created between the considered spherulites are obtained by the modification of eq (12). The procedure described in refs. 16 and 17 can be applied for the purpose. The substitution $r = r(\tau_1, t)$, followed by integration over the range $0 < \tau_2 < t$ and for $n = 3$, also over $0 < \tau_3 < t$, gives us the probability that the arbitrarily chosen point will become the boundary between n spherulites at a distance r from this center, which was nucleated at τ_1. t is defined now by the relation

$$\int_{\tau_1}^t G(t')\,dt' = r \tag{14}$$

which for isothermal crystallization assumes the simple form $t = \tau_1 + r/G$.

For $n = 3$, division of the result by $(n - 1)!$ is necessary to avoid multiple counting of the same events. To obtain the probability that point A will become a boundary between two or three spherulites at a distance r from one of the centers, the integration over $0 < \tau_1 < \infty$ is required.

Finally, the distributions of distances from spherulite centers to the boundaries of the considered spherulites at distances s_1 and s_2 from the sample borders are in the form

$$R_2(r, s_1, s_2)\, dr = r\left\{\int_0^\infty F(\tau_1)\exp\left[-\int_0^t F(\tau)S[r(\tau, t), s_1, s_2]\, d\tau\right] \times \int_0^t F(\tau_2)r(\tau_2, t)V_2(\tau_1, \tau_2)\, d\tau_2 d\tau_1\right\} dr \quad (15a)$$

$$R_3(r, s_1, s_2)\, dr = (2!)^{-1}r\left\{\int_0^\infty F(\tau_1)\exp\left[-\int_0^t F(\tau)S[r(\tau, t), s_1, s_2]\, d\tau\right] \times \int_0^t \int_0^t F(\tau_2)r(\tau_2, t)F(\tau_3)r(\tau_3, t)V_3(\tau_1, \tau_2, \tau_3)\, d\tau_3 d\tau_2\, d\tau_1\right\} dr \quad (15b)$$

where t is defined by eq. (14).

Assuming $F(t) = D\delta(t)$, where δ is the Dirac delta function, one can use eqs. (13) and (15) to calculate the rates of boundaries formation and also the distributions of distances from centers to boundaries for the instantaneous nucleation.

As it follows from the formulas derived on the basis of the probabilistic model, the sample limits influence the development of interspherulitic boundaries at time t within a distance $r = \int_0^t G(t')\, dt'$. In the case of more intense nucleation of spherulites, the crystallization ends faster; hence, the sample limits influence the structure formation within the shorter distance.

To obtain the rates of boundaries formation and the distance distributions from centers to boundaries in the entire strip, one has to perform integration over the range $0 < s_1 < h$ and to divide the result by h

$$H_{av}(t, 2h) = h^{-1}\int_0^h H(t, s_1, 2h - s_1)\, ds_1 \quad \text{and}$$

$$R_{av}(r, 2h) = h^{-1}\int_0^h R(r, s_1, 2h - s_1)\, ds_1 \quad (16)$$

The boundary length, $L_2(t, 2h)$, and the number of boundary points, $L_3(t, 2h)$, formed until time t can be also obtained by the respective integration

$$L_n(t, 2h) = h^{-1}\int_0^t \int_0^h H_n(t', s_1, s_2)\, dt_1 \quad \text{for} \quad n = 2 \quad \text{and} \quad n = 3 \quad (17a)$$

The length of interspherulitic lines and the number of triple points per unit area of a sample after a completion of crystallization are equal to $L_2(\infty, 2h)$ and $L_3(\infty, 2h)$, respectively. To obtain the number of boundaries at given time per a spherulite, one has to divide L_2 and L_3 by the number of spherulites in unit area, N[10]:

$$N(2h) = \int_0^\infty F(t')[1 - \alpha(t', 2h)]\, dt' \quad (17b)$$

where $\alpha(t')$ is a conversion degree at time t'[10]:

$$\alpha(t', 2h) = 1 - h^{-1} \times \int_0^h \exp\left[-\int_0^{t'} F(\tau)S[r(\tau, t), s_1, 2h - s_1]\, d\tau\right] ds_1 \quad (17c)$$

The rate of boundaries formation and the distributions of distances from centers to boundaries in an infinite sample are directly obtained from the respective expressions by neglecting the sample limits, that is, assuming that S equals πr^2 and that each spherulite can be nucleated within an angle $(0, 2\pi)$ around the boundary point. This leads to the respective expressions in the following form:

$$H_{n\infty}(t)\, dt = C_n\exp\left\{-\pi\int_0^t F(\tau)[r(\tau, t)]^2\, d\tau\right\} \times \left[\int_0^t F(\tau)r(\tau, t)\, d\tau\right]^n (n!)^{-1}G(t)\, dt \quad (18a)$$

$$R_{n\infty}(r)\, dr = C_n\, r dr\, [(n - 1)!]^{-1} \times \int_0^\infty F(\tau_1)\exp\left\{-\pi\int_0^t F(\tau)[r(\tau, t)]^2\, d\tau\right\} \times \left[\int_0^t F(\tau)r(\tau, t)\, d\tau\right]^{n-1} d\tau_1 \quad (18b)$$

where $C_2 = 16\pi$ and $C_3 = 24\pi^2$.

The amounts of boundaries between n spherulites per unit area of infinite film formed until time t, $L_{n\infty}(t)$, can be obtained by the integration of $H_{n\infty}(t')$ over the range $0 < t' < t$.

Equation [18(a,b)] is similar to the respective formulas derived in refs. 17–19, except for the coefficient C_n (C_2 and C_3) and differs by the factors $4/\pi$ and $3/\pi$, respectively, from the corresponding coefficients in refs. 17–19. Equation [18(a,b)] leads, therefore, to the identical form of the normalized distributions but to somewhat different amounts of boundaries per sample unit area, compared with those calculated in refs. 17–19.

For the constant ratio of nucleation rate to growth rate: $F(t)/G(t) = Q =$ constant, the amount of boundaries per unit area depend on Q and on film width only.

The improved way of derivations demonstrated here allows us to reproduce correctly the computer simulation and experimental results concerning the influence of the sample limits on the development and the final form of the spherulitic pattern. For the infinite film instantaneously nucleated, the improved model predicts the length of lines surrounding an average spherulite, $2L_{2\infty}/N$, equal to $4N^{-0.5}$, which is typical for tetragonal packing. The number of triple boundary points at the average spherulite circumference, $3L_{3\infty}/N$, in an infinite film is independent of the nucleation and equals 6, as in the case of hexagonal packing.

To demonstrate the influence of the borders of thin film on the development of the spherulitic pattern, we calculated the rates and the progression of boundaries formation and the distributions of distances from spherulite centers to boundaries according to formulas derived in this section for both instantaneous nucleation and time-dependent nucleation. In the latter case, the total number of potential nuclei in a polymer melt equaled N_0, and they showed up at a rate that decreased exponentially with time: $F(t') = qN_0 \exp(-qt')$. The following data were used: $G = 5$ unit/min, $D = 6.25 \times 10^{-4}$ unit^{-2}, $q = 0.5$ min^{-1}, and $N_0 = 0.001$ unit^{-2}. The selected parameters ensured similar numbers of spherulites per unit surface in the infinite sample, independently of the nucleation. We also calculated the conversion degree and the distributions of distances from spherulite centers to the internal points of these spherulites (i.e., points confined to the area between boundaries formed by the considered spherulite with its neighbors) for both the infinite and finite samples, taking advantage of formulas derived in refs. 10, 11, and 17–19. In addition, the total number of spherulites, the total length of the boundary lines, and the number of triple points per unit area were computed.

To compare the experimental results concerning POM films to the model predictions, we also performed calculations for nucleation rate constant with time. The number of spherulites per unit area in the infinite film in this case depended entirely on the ratio of nucleation rate to growth rate, Q, in the following way[18,19] $N = (\pi Q/3)^{1/3}\ \pi^{-1}\Gamma(1/3)$, where $\Gamma(x)$ denotes the gamma function. From the number of spherulites per unit area of the wide POM film, a Q value equal to 113.22 mm^{-3} was obtained and then used for calculation of the number of triple points and the length of interspherulitic boundary lines per unit area in the wide and narrow POM samples. The number of spherulites per unit area in the narrow strip of POM was also calculated.

COMPUTER SIMULATION

Computer simulation is a way to verify such model, provided that it accounts for the same basic assumption as the model.

In our case, we used a previously developed software,[21,22] aiming at reproducing the crystallization of the polymers. The two-dimensional version of the software was used. The sample is assumed to be a rectangle of finite width, $2h$, and length, L. Crystallization resulted, then, of the nucleation and the growth of circular entities. The nucleation was represented through the concept of potential nuclei, whose initial density was N_0 per unit surface. The nuclei could be activated according to a given activation frequency, q. The activation rate was then given by $\nu(t) = 2hLN_0q \exp(-qt)$.

A nucleus, located in a still liquid zone, could be activated, whereas a nucleus that was overlapped by an older spherulite before its activation could not be activated. So, the actual appearance rate of spherulites was always lower than or equal to ν. The growth rate was equal for all entities, and growth began immediately after activation. The activation rate was imposed on an average. That is, time was decomposed into fictitious increments having a $1/\nu(t)$ duration. That is, the first spherulite to appear had to appear between time 0 and the time $t = 1/\nu(0)$. Its precise activation time was chosen at random within this time increment. Its location was also chosen at random. For these two purposes, the random number generator of the computer was used. Successive nucleation of the n^{th} entity was then controlled in the same way. The exact time of nucleation was chosen at random between time t_{n-1} and t_n defined as $t_{n-1} + [1/\nu(0)]$. Location was always chosen at random on the entire surface of the specimen, but from the second nucleation to last one, this location had to be tested. If this point was still in a liquid region, a new spherulite appeared; if not, no spherulite was generated, and the following time increment was considered. Instantaneous nucleation was modeled through a high value of q, which made all the entities appear at approximately the same time. Consequently, at a given time, a given set of spherulites existed and had (each of them) a given maximum radius. Locations and times of the appearance of any possible triple points were simply deduced from the locations and the times of

nucleation of the spherulites. Two coordinates and a time of appearance represented each of these points. Once again, the only existing triple points were those that appeared in a still liquid zone. Then, boundaries were calculated to account for the following considerations:

- Spherulites had to be close enough to each other to develop a boundary.
- For given set of two spherulites, the first potential point of the boundary was located on the same straight line as the two centers.
- Then, the potential boundary could develop in two directions apart from this point. The locations of successive points were calculated by discretizing time from the moment of appearance of the first point of contact to either the current time, or the closest triple point involving both the two considered spherulites, or the boundary of the sample or a liquid zone (defining here the last boundary point).
- If the contact point could not appear (due to its previous solidification), the first points of the boundary to be considered were the two closest triple points involving both considered entities. Calculations were then performed in the same way as before.
- In the case of incomplete crystallization, circular solid versus liquid boundaries existed between given last boundary points, except if these circles intercepted the specimen boundaries.

With this method, it was possible to calculate at the same time the number and the location of existing spherulites, triple points, and boundary points. The surface of all entities and the length of all boundary lines were then cumulated.

When computer simulations were used, depending on the position of nuclei and their instant of activation, the crystallization kinetics of the fictitious sample varied from one calculation to another. Conversely, theoretical models led to average values. To make these two kinds of approach comparable, we had to perform several runs of simulations for each set of parameters and then average their results. In our case, we performed at least 500 runs per simulation, being cautious that the random generations were significantly different. Additionally, to make our results as representative as possible, we made the length of the fictitious sample sufficiently high to make the sample contain at least 100 spherulites. All of this protocol was defined during preliminary work.

RESULTS OF MODELING

The conversion degree and the progression of the formation of interspherulitic boundaries, lines, and

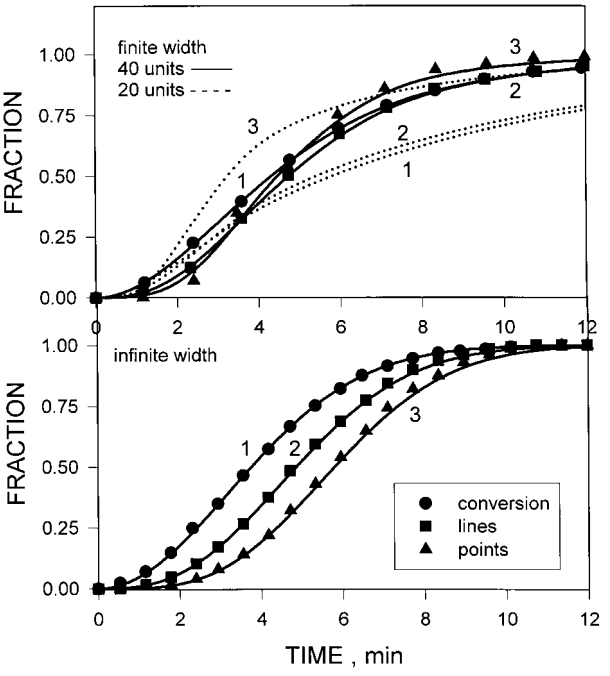

Figure 6 (1) Conversion degree and the progression of (2) boundary lines and (3) triple point formation against time in finite and infinite samples crystallizated from instantaneous nuclei. Symbols denote the results of computer simulation in the case of the 40 unit width sample and the infinite sample.

triple points in the finite and infinite strips of film are plotted in Figures 6 and 7 for the instantaneous nucleation and for the nucleation at a rate that decreased exponentially with time. The average spherulite radius in the infinite film was 22.6 units in the case of the instantaneous nucleation and 19.4 units for the nucleation at a rate decreasing exponentially with time. The symbols that denote the results of computer simulation follow the curves calculated on the basis of the probabilistic model, thus indicating good agreement between the predictions of these two methods.

Although in the infinite sample the boundaries kinetics were always slower than the conversion rate, in the narrow strips the progression of the formation of interspherulitic lines became similar to the conversion of melt into spherulites. The formation of triple points for its part became faster than the conversion. The decrease of sample width eliminated the boundaries and even more of the triple points that appeared at late stages of crystallization. The changes in boundaries formation kinetics are clearer in Figure 8, where the length of lines and the number of triple points in unit area of film per unit time are drawn against time for the infinite sample and the narrow strips. The formation of the triple points and especially of the interspherulitic boundary lines lasted longer in the narrow strips than in the infinite film, which was associated with the slower conversion of melt in spherulites in such strips. The decrease of sample

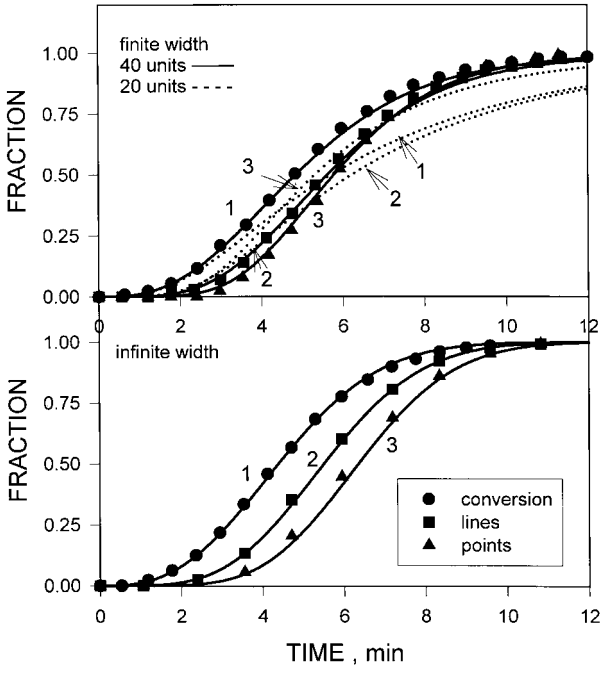

Figure 7 (1) Conversion degree and the progression of (2) boundary lines and (3) triple point formation against time in finite and infinite samples. Crystallization was with nucleation at a rate exponentially dependent on time. Symbols denote the results of computer simulation in the case of the 40 unit wide sample and the infinite sample.

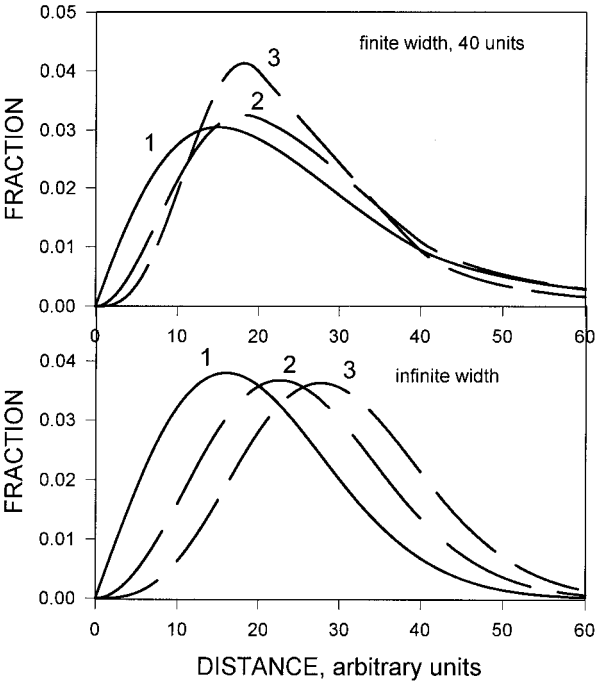

Figure 9 Distributions of distances from spherulite centers to spherulite (1) internal points, (2) interspherulitic lines, and (3) triple points in finite and infinite samples crystallized instantaneous nuclei.

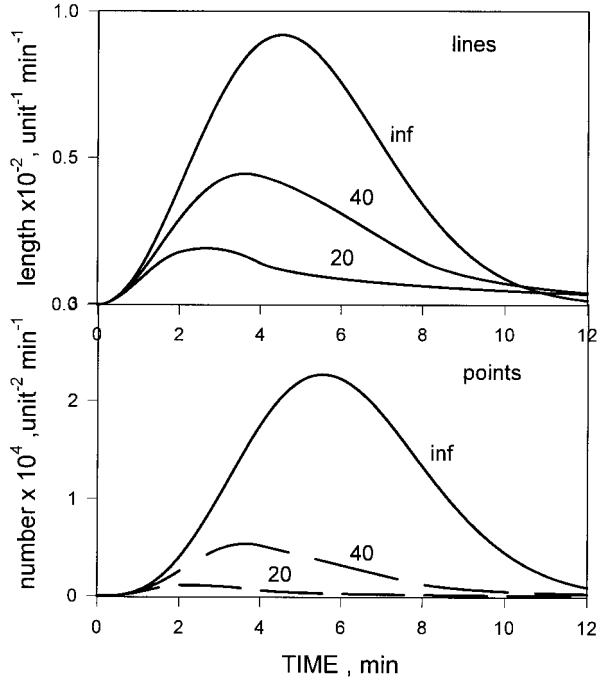

Figure 8 Rates of formation of boundary lines and triple points between spherulites in instantaneously nucleated finite and infinite samples. Numbers denote the width of finite samples expressed in arbitrary units.

width could not eliminate the interspherulitic boundary lines to such extent as the triple impingement points because the interspherulitic lines were always formed when two crystallization fronts met. Hence, the slower conversion in the narrow strip caused the formation of interspherulitic boundary lines in the strip to last longer not only than in the infinite samples but also longer than the formation of triple points in the same strip. In the case of sporadic nucleation, the effect of the decrease in the sample width on the formation of interspherulitic boundaries was less pronounced than in the instantaneous nucleation.

The sample width also influenced the distance distributions (Figs. 9 and 10). Although in the infinite samples the distributions of distances from spherulite centers to boundaries were shifted toward longer distances as compared with distributions of distances from spherulites centers to internal points of spherulites, the decrease of the sample width changed this tendency. The normalized distributions of distances from the spherulite centers to triple points for the finite width samples had larger fractions of short distances than those for the infinite films. The maxima of the distributions of distances from the centers to interspherulitic boundary lines and to triple points in the narrow strips were shifted toward shorter distances as compared with the respective functions for the infinite samples. Nevertheless, the distributions of distances to interspherulitic lines had tails extending toward the longer distances, which resulted from the

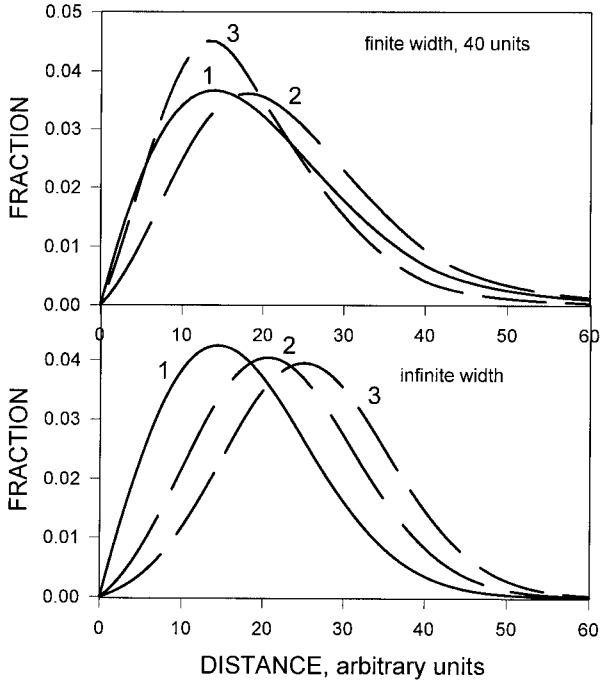

Figure 10 Distributions of distances from spherulite centers to spherulite (1) internal points, (2) interspherulitic lines, and (3) triple points in finite and infinite samples. Crystallization was with the nucleation at a rate exponentially dependent on time.

impingement of spherulitic fronts at the late stages of respectively slow crystallization in the narrow strips.

The length of interspherulitic lines and the number of triple points per unit area of sample against sample width is plotted in Figure 11. In both cases, the instantaneous nucleation and the nucleation at a rate exponentially dependent on time, the amount of interspherulitic boundaries in unit area decreased with the sample width, especially for sample widths smaller than the diameter of the average spherulite. Even in the samples having the width on an order of several spherulite diameters, the number of triple points in unit area was lower by a few percentage points than that in the infinite film. The number of triple points in unit area in the instantaneously nucleated semi-infinite sample is plotted against distance from sample edge in Figure 12. The average number of points within this distance is also drawn in Figure 12. Although the local number of points per unit area rose fast with a distance from the sample edge, the increase of the average value was slower. Hence, even in wide samples, the number of triple points per unit area could be lower than the number calculated for an infinite film. The effect of sample edges on the spherulitic boundaries was less pronounced for the sporadic nucleation. However, in this case, the number of spherulites per unit area of sample increased, as shown in Figure 11. The reason for this was the slower conversion of melt into spherulites, which allowed more nuclei to appear.

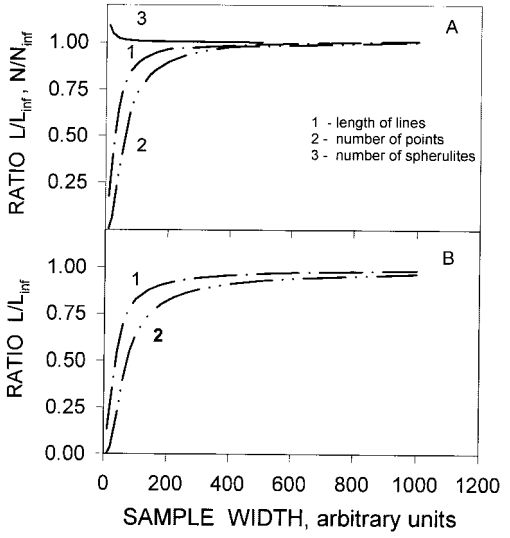

Figure 11 The length of boundary lines (1), the number of triple points (2), and the number of spherulites (3) in unit area of the finite width sample divided by the respective values of the infinite sample: (A) nucleation at a rate dependent exponentially on time and (B) instantaneous nucleation.

Although we do not know the exact time dependence of nucleation in the POM film, some of the boundaries between spherulites were curvilinear, which suggests sporadic nucleation. The calculations of the length of interspherulitic boundaries and the number of triple points in unit area of the infinite film and as in unit area of the narrow strip were based on the constant ratio of nucleation rate to growth rate, Q, as determined from the number of spherulites per unit area measured for the wide POM film. The obtained values for the length of boundaries were 6.65 and 4.82 mm^{-1}, whereas the number of triple points were 43.1 and 20.14 mm^{-2} for the infinite film and for the strip of width of 0.24 mm, respectively. The calculated

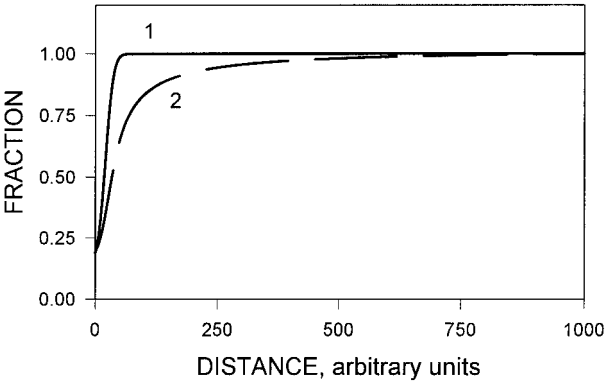

Figure 12 Progression of number of triple points per unit area in the instantaneously nucleated semi-infinite sample against distance from edge: (1) local number of points at a given distance and (2) average number of points in a region adjacent to sample edge, from edge to a given distance.

number of spherulites per unit area of the narrow strip was 23.6 mm^{-2}. Thus, the model predicted in the narrow strip of POM the increase of the number of spherulites to 1.15 and the decrease in boundary length and the triple points number to 0.72 and to 0.47, respectively, of the equivalent values in the infinite film of the same area. The respective data obtained experimentally were as follows: the spherulite number increased to 1.23, whereas the length of lines decreased to 0.75 and the number of triple points number decreased to 0.41 of the values measured for the wide POM film. Having in mind that we do not know the exact nucleation rate time dependence in the POM sample, we can conclude that the probabilistic model allowed us to predict at least in a qualitative way the changes in microstructure related to sample finite width. The distributions of distances from spherulite centers to triple points determined for the POM samples indicated the larger fraction of short distances in the narrow strip of POM than in the wide sample, which was also predicted by the probabilistic model.

DISCUSSION

In this study, the changes of isothermally crystallized two-dimensional spherulitic structure due to the presence of spatial limits were evaluated by means of the experimental measurements, computer simulation, and a probabilistic model.

The results obtained clearly indicate that the spatial limits of the polymer portion influenced the spherulitic structure. The regions adjacent to the polymer borders differed considerably from the polymer interior. The effects were significant within a distance comparable with the average spherulite size. Thus, the decrease in the film width influenced the spherulitic structure and led to a diminished number of interspherulitic boundaries and, if the nucleation lasted in time, to the increased number of spherulites in unit area. The process of the formation of triple points and especially of interspherulitic boundary lines lasted longer in narrow strips of film than in films of infinite width. Some interspherulitic lines were formed in the large distances from spherulite centers at the late stages of crystallization. There was no direct relation between the kinetics of the formation and the final form of the spherulitic structure in narrow strips of polymer and in wide films.

Although the results obtained on the basis of the probabilistic model described in this article concern isothermal crystallization, the general formulas are valid for the isothermal and nonisothermal processes. Often, additional nucleation occurs on polymer borders if they are in contact with foreign surfaces having the ability to nucleate the polymer crystallization. Such effects were not accounted for in the present article, nevertheless, both the probabilistic model and the computer simulation methods described have the potential ability to deal with this problem.

Although only the two-dimensional spherulitic crystallization was studied, one can expect similar tendencies in changes of spherulitic structure formation and in its final form due to the spatial limits of a polymer also in three dimensions. Thin polymer films are frequently used to study the spherulitic structure of a polymer. The thin film is, in fact, a confined portion of polymeric material, and its structure is not representative for a bulk. In the case of nucleation prolonged in time, the number of spherulites in unit volume of thin film might be different than in bulk even in the absence of additional nucleation at film surfaces. Because the nucleation and growth of spherulites depend on crystallization temperature, the effect of film thickness on the spherulite number and also on the spherulitic pattern can vary with temperature, obscuring to some extent the relations between the nucleation, the spherulitic structure, and the temperature found for the polymer investigated.

CONCLUSIONS

In this article, we have shown experimentally, by means of the computer simulation, and also by the probabilistic model of spherulite nucleation and growth that the spatial limits of a polymer influence not only the conversion of melt into spherulites but also the spherulitic structure. The progression of interspherulitic boundaries formation and the final spherulitic pattern are affected by the sample borders. If the primary nucleation is sporadic in time, the number of spherulites per unit area increases. The length of the interspherulitic lines and the number of impingement points per unit area diminishes independently of nucleation, although the effect is the strongest when spherulites are instantaneously nucleated. Thus, the regions adjacent to sample borders are not representative for the bulk spherulitic structure.

APPENDIX A

For $\tau_1 > \tau_2$

$$V_2(\tau_1, \tau_2) = 2\{4(\beta_1 - \alpha_1) - 8 \sin[0.5(\beta_1 - \alpha_1)] + q(\alpha_2, \alpha_1, \alpha_1, \beta_1) + q(\alpha_1, \beta_1, \beta_1, \beta_2) + q(\alpha_1, \beta_1, \alpha_2', \beta_2')\}$$

where

$$q(\omega_0, \omega_k, \theta_0, \theta_k) = 4\{\sin[0.5(\theta_k - \omega_k)] + \sin[0.5(\theta_0 - \omega_0)] - \sin[0.5(\theta_k - \omega_0)] - \sin[0.5(\theta_0 - \omega_k)]\}$$

For $\tau_1 > \tau_2 > \tau_3$

$$V_3(\tau_1, \tau_2, \tau_3) = 2\{6[(\beta_1 - \alpha_1)^2/4 + \cos(\beta_1 - \alpha_1) - 1 + 0.25(\beta_1 - \alpha_1)\sin(\beta_1 - \alpha_1)] + rx(\alpha_3, \alpha_2, \alpha_2, \alpha_1, \alpha_1, \beta_1) + rx(\alpha_2, \alpha_1, \alpha_1, \beta_1, \beta_1, \beta_3) + rx(\alpha_3, \alpha_2, a_2, \alpha_1, \alpha_1, \beta_1) + rx(\alpha_2, \alpha_1, \alpha_1, \beta_1, \beta_1, \beta_3) + re(\alpha_1, \beta_1, \alpha_2, \alpha_1) + re(\alpha_2, \alpha_1, \alpha_1, \beta_1) + re(\alpha_3, \alpha_1, \alpha_1, \beta_1) + re(\beta_1, \beta_3, \alpha_1, \beta_1) + re(\beta_1, \beta_2, \alpha_1, \beta_1) + re(\alpha_1, \beta_1, \beta_1, \beta_2) + rx(\alpha_2, \alpha_1, \alpha_1, \beta_1, \alpha_3', \beta_3') + rx(\alpha_1, \beta_1, \beta_1, \beta_2, \alpha_3', \beta_3') + re(\alpha_3', \beta_3', \alpha_1, \beta_1) + rx(\alpha_3, \alpha_1, \alpha_1, \beta_1, \alpha_2', \beta_2') + rx(\alpha_1, \beta_1, \beta_1, \beta_3, \alpha_2', \beta_2') + re(\alpha_2', \beta_2', \alpha_1, \beta_1) + rx(\alpha_1, \beta_1, \alpha_3', \alpha_2', \alpha_2', \beta_2') + rx(\alpha_1, \beta_1, \alpha_2', \beta_2', \beta_2', \beta_3') + re(\alpha_1, \beta_1, \alpha_2', \beta_2')\}$$

where

$$re(\omega_0, \omega_k, \gamma_0, \gamma_k) = 0.25\{(\gamma_k - \gamma_0)[\sin(\omega_k - \gamma_0) - \sin(\omega_0 - \gamma_0) - \sin(\gamma_k - \omega_k) + \sin(\gamma_k - \omega_0)] + [(\gamma_k - \gamma_0) - \sin(\gamma_k - \gamma_0)](\omega_k - \omega_0)\} + 0.5[\cos(\gamma_k - \omega_0) - \cos(\gamma_0 - \omega_0) + \cos(\gamma_0 - \omega_k) - \cos(\gamma_k - \omega_k)]$$

$$rx(\omega_0, \omega_k, \theta_0, \theta_k, \gamma_0, \gamma_k) = 0.25\{(\gamma_k - \gamma_0)[\sin(\theta_k - \omega_k) - \sin(\theta_k - \omega_0) - \sin(\theta_0 - \omega_k) + \sin(\theta_0 - \omega_0)] + (\theta_k - \theta_0)[\sin(\gamma_{0^-}\omega_k) - \sin(\gamma_{0^-}\omega_0) - \sin(\gamma_{k^-}\omega_k) + \sin(\gamma_{k^-}\omega_0)] + (\omega_k - \omega_0)[\sin(\gamma_k - \theta_k) + \sin(\gamma_0 - \theta_0) - \sin(\gamma_k - \theta_0) - \sin(\gamma_0 - \theta_k)]$$

APPENDIX B

Let us consider a plane with randomly distributed points. The probability, P, that n points will be found in the area V_s is expressed by the Poisson probability distribution: $P = \exp(-D_sV_s)(D_sV_s)^n/n!$, where D_s denotes the average density of points. If n points are within the area V_s then P represents the probability that the average density of points on the plane equals D_s. P is a bell-shaped function with a maximum at $D_s = n/V_s$ and has the width dependent on D_s and n. The probability that the average density of points is between D_1 and D_2 can be calculated by the integration of P over the range $D_1 < D_s < D_2$. We are aware that neither the triple points nor the spherulite centers in the case of prolonged nucleation are entirely randomly distributed in polymer films, but they are somewhat correlated on short distances.[16,19,23] Nevertheless, this should not affect the number of centers and triple points in comparatively large areas of the wide film and of the narrow strips.

The calculations conducted for spherulite centers led to the conclusion that the probability for the average density of centers in the wide film to exceed the determined value of 20.28 mm^{-2} by more than 10% was .05. The density of centers in the narrow strip could be lower than 10% of the value of 25.38 mm^{-2} with the probability of .15. Thus, the probability of simultaneous occurrence of both events was lower than .01. The probability that the average density of triple points in the narrow strip surpassed the value of 16.24 mm^{-2} by 10% was .26, but the average density of points in the wide film could be lower than 10% of 39.75 mm^{-2} with the very small probability of .012 only. The probability that the average densities of triple points in both samples were within the same range of values was infinitely small.

References

1. Schultz, J. M. Polym Eng Sci 1984, 24, 770.
2. Mucha, M.; Kryszewski, M. Colloid Polym Sci 1980, 258, 743.
3. Avrami, M. J Chem Phys 1939, 7, 1103; 1940, 8, 212; 1941, 9, 177.
4. Evans, U. R. Trans Faraday Soc 1945, 41, 365.
5. Ozawa, T. Polymer 1971, 12, 150.
6. Nakamura, K.; Katayama, K.; Amano, T. J Appl Polym Sci 1973, 17, 1031.
7. Escleine, J. M.; Monasse, B.; Wey, E.; Haudin, J. M. Colloid Polym Sci 1984, 262, 366.
8. Billon, N.; Escleine, J. M.; Haudin, J. M. Colloid Polym Sci 1989, 267, 668.
9. Billon, N.; Haudin, J. M. Colloid Polym Sci 1989, 267, 1064.
10. Piorkowska, E. Colloid Polym Sci 1997, 275, 1035.
11. Piorkowska, E. Colloid Polym Sci 1997, 275, 1046.
12. Billon, N.; Magnet, C.; Haudin, J. M.; Lefebvre, D. Colloid Polym Sci 1994, 272, 633.
13. Piorkowska, E. Macromol Symp 2001, 169, 143.
14. Mehl, N. A.; Rebenfeld, L. J Polym Sci Part B: Polym Phys 1993, 31, 1677.
15. Mehl, N. A.; Rebenfeld, L. J Polym Sci Part B: Polym Phys 1993, 31, 1687.
16. Piorkowska, E.; Galeski, A. J Polym Sci Polym Phys Ed 1985, 23, 1273.
17. Piorkowska, E. J Chem Phys 1995, 99, 14007.
18. Piorkowska, E. J Chem Phys 1995, 99, 14016.
19. Piorkowska, E. J Chem Phys 1995, 99, 14024.
20. Galeski, A.; Koenczoel, L.; Piorkowska, E.; Baer, E. Nature 1986, 325, 40.
21. Billon, N.; Haudin, J. M. Ann Chem Fr 1990, 15, 1.
22. Billon, N.; Monasse, B.; Haudin, J. M.; Chenot, J. L. In Computer Aided Training in Science and Technology; Onate, E.; Suarez, B.; Owen, D. R. J.; Schrefler, B.; Kroplin, M.; Kleiber, M., Eds.; CIMNE, Pineridge Press: Barcelona, 1990; p 384.
23. Galeski, A.; Piorkowska, E. J Polym Sci Polym Phys Ed 1983, 21, 1299.